J Fluoresc (2017) 27:1747–1758
DOI 10.1007/s10895-017-2113-3

ORIGINAL ARTICLE

Benzocoumarin-Styryl Hybrids: Aggregation and Viscosity Induced Emission Enhancement

Umesh Warde[1] · **Nagaiyan Sekar**[1]

Received: 15 January 2017 / Accepted: 8 May 2017 / Published online: 12 May 2017

Abstract Two benzo[h]chromen-3-yl)ethylidene) malononitrile styryl hybrid dyes are synthesized and characterized by NMR and elemental analysis. One is based on nitrogen donor and other on oxygen (**3b** and **3b** respectively**)**. Dyes are low emissive in the solution but dramatically showed increase in emission intensity in aggregates form in the THF **(**tetrahydrofuran**)** /water system. Dyes are also sensitive to viscosity and showed increased emission intensity in the DCM:PEG 400 system and DMF:PEG 400 system respectively. Dyes **3a** and **3b** showed higher viscosity sensitivity constant (0.67 and 0.39 respectively) in DMF:PEG 400 system compared to DCM:PEG 400 (0.47 and 0.21 respectively) system which is contrary to the traditional concept of FMRs. Results shows that lowering of twisted intramolecular charge transfer (TICT) and increase in intramolecular charge transfer (ICT) in the excited state could be the reason for such behavior in the aggregate and highly viscous state. This study may provide the new insights into the field of AIEE and FMR research of such hybrid molecules.

Keywords Coumarin-styryl hybrids · ICT · TICT · AIEE · FMR

Electronic supplementary material The online version of this article (doi:10.1007/s10895-017-2113-3) contains supplementary material, which is available to authorized users.

✉ Nagaiyan Sekar
n.sekar@ictmumbai.edu.in; nethi.sekar@gmail.com

[1] Department of Dyestuff Technology, Institute of Chemical Technology, N. P. Marg, Matunga, Mumbai, (MH) 400019, India

Introduction

Luminogens with properties like aggregation induced emission (AIE) or enhanced emission (AIEE), fluorescent molecular rotors (FMR) are of great interest in modern age research [1–3]. The compounds having AIE properties have been studied for fluorescence sensors (for explosive, ion, pH, temperature, viscosity, pressure, etc.), biological probes (for protein, DNA, RNA, sugar, phospholipid, etc.), immunoassay markers, PAGE visualization agents, polarized light emitters, monitors for layer-by-layer assembly, reporters for micelle formation, multi stimuli-responsive nanomaterials, and active layers in the fabrication of organic light-emitting diodes [4–8]. Fluorescent compounds as molecular rotors have found a wide range of applications as fluorescent sensors of microviscosity and solvent free volume, bulk viscosity measurement, probing dynamics of polymer formation, protein sensing and probing of protein aggregation, and microviscosity probing in living cells [9–12].

Coumarins and styryls are two classes of fluorophores which have been studied the most for above mentioned properties [13, 14]. This is because these two classes have donor-pi-acceptor (D-π-A) systems most of the times and shows intramolecular charge transfer (ICT). ICT is the most important criteria for above mentioned properties because it directs the luminosity of the excited state [15, 16]. If the excited state is planar and sufficiently populated, luminescence observed. The luminescence diminishes if intramolecular rotation is favored by the solvent interactions which disturbs the planarity and eventually ICT which undergoes twisted intramolecular rotation (IR) leading to TICT which opens the gate for non-radiative decays [17]. In TICT complexes, the major energy loss is because of the dominant vibrational state due to the formation of the twisted state [18]. The unbalanced dipole moments upon photon

absorption causes twisting of the molecules to stabilize the dipole moment or other in words smooth charge transfer [18]. This requires the ability of the donor atom (nitrogen or oxygen) in the donor group to undergo a change from a ground state conformation (pyramidal in case of nitrogen) to a planar conformation in the charge transfer state. Thus it can be sensed that, in the medium where this twisting due to the intramolecular rotation is avoided, the luminescence increases [19]. The AIE luminogens in solid state are perfectly aligned in plane in the crystal packing and smooth ICT takes place without or minimum TICT [15, 20]. This increases the emission intensity of luminogens which is also applicable in the aggregate state where molecules get arranged in the restricted planar geometry in the crystals and show increased emission [21, 22]. Similarly, the molecular rotors property i.e. viscosity sensing is only plausible if TICT is operating in the system [23]. Many long conjugated molecules with twisted skeleton conformation have been established to show AIE phenomenon [6]. The restriction of the intramolecular rotation (RIR) and the non-planar conformation with π-π stacking interactions are mainly responsible for the AIE effect [24]. In the similar manner, viscosity sensing can be appreciated if TICT is present and inhibition of which increases the emission intensity [23].

The coumarin-styryl hybrid dyes can provide all these geometrical parameters to achieve aforementioned properties. They have extended conjugation with one or sometimes two donor or acceptor groups in the molecular framework [25]. The vast literature on these kind of dyes is the evidence of their importance for advanced studies such as AIEE and FMRs. Such molecules have been widely synthesized and studied for biological purposes [26, 27]. Many fluorescent compounds having extended styryls fused with coumarins have been developed and studied for their fluorescence properties [28–30]. It is evident that some substituents makes these molecules more interesting as cyano coumarins known for their red shifted fluorescence [31–33]. Many coumarin-styryl hybrids having cyano group as extension have also been studied for their red shifted fluorescence [34, 35]. It is also known that many fluorescent compounds having cyano group as substituent have been developed and studied for its effects on emission properties. Cyano group has been frequently utilized as a functional unit in the design of advanced optical materials because of it's the structural simplicity and high polarizability. As a result, a great number of AIE luminogens containing cyano groups have been developed and reported because its restricted motion enhances the ICT and thus fluorescence increases [1, 36]. Both steric and electronic effects of a cyano group affect the emission process of an AIE luminogen. The steric effect of a cyano group on the conformation of an AIE luminogen can be readily appreciated [20, 37]. Cyano group is known for its crucial role in FMRs also [37].

On this line, we have developed the 3-styryl coumarins as hybrids of coumarins (**3a** and **3b)** having different donor and cyano groups as extended part of conjugations. These molecules are studied for their absorption and emission properties in solvents of different polarities. They are found to be very weakly fluorescent in the solution. Compounds **3a** and **3b** were found **to be** AIE as well as FMR active compounds. As structural features are very important for AIEE and FMR properties, we studied the geometries of the dyes in the ground state as well as in the excited state with help of the DFT optimized structures using B3LYP method and 6-31G(d) basis set (Figs. 1, 2 and 3).

Materials and Methods

All the commercial reagents were procured from SD Fine Chemicals (Mumbai) and were used without further purification. Laboratory reagent grade solvents were purchased from Rankem, Mumbai. The reactions were monitored by TLC using on 0.25 mm EMerck silica gel 60 F_{254} precoated plates, which were visualized using UV light (254 nm and 344 nm). Melting points were measured on standard melting point apparatus from Sunder Industrial products, Mumbai and are uncorrected. Proton and Carbon NMR spectra were recorded on Varian 500 MHz instrument using TMS as an internal standard. Mass spectra were recorded on FINNIGAN LCQ ADVANTAGE MAX instrument from Thermo Electron Corporation (USA). The absorption spectra of the compounds

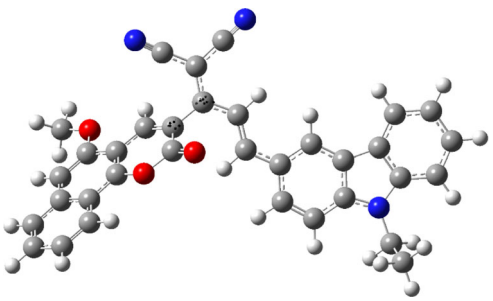

Dye **3a** in THF (ground state)

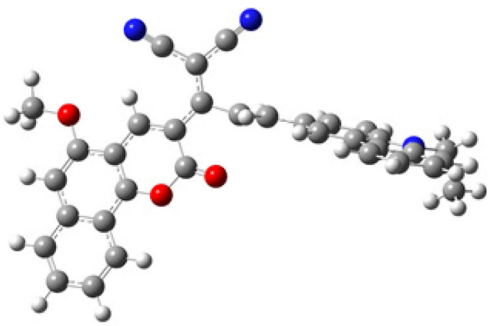

3a in THF (excited state)

Fig. 1 DFT optimized structures of the dye **3a** in THF

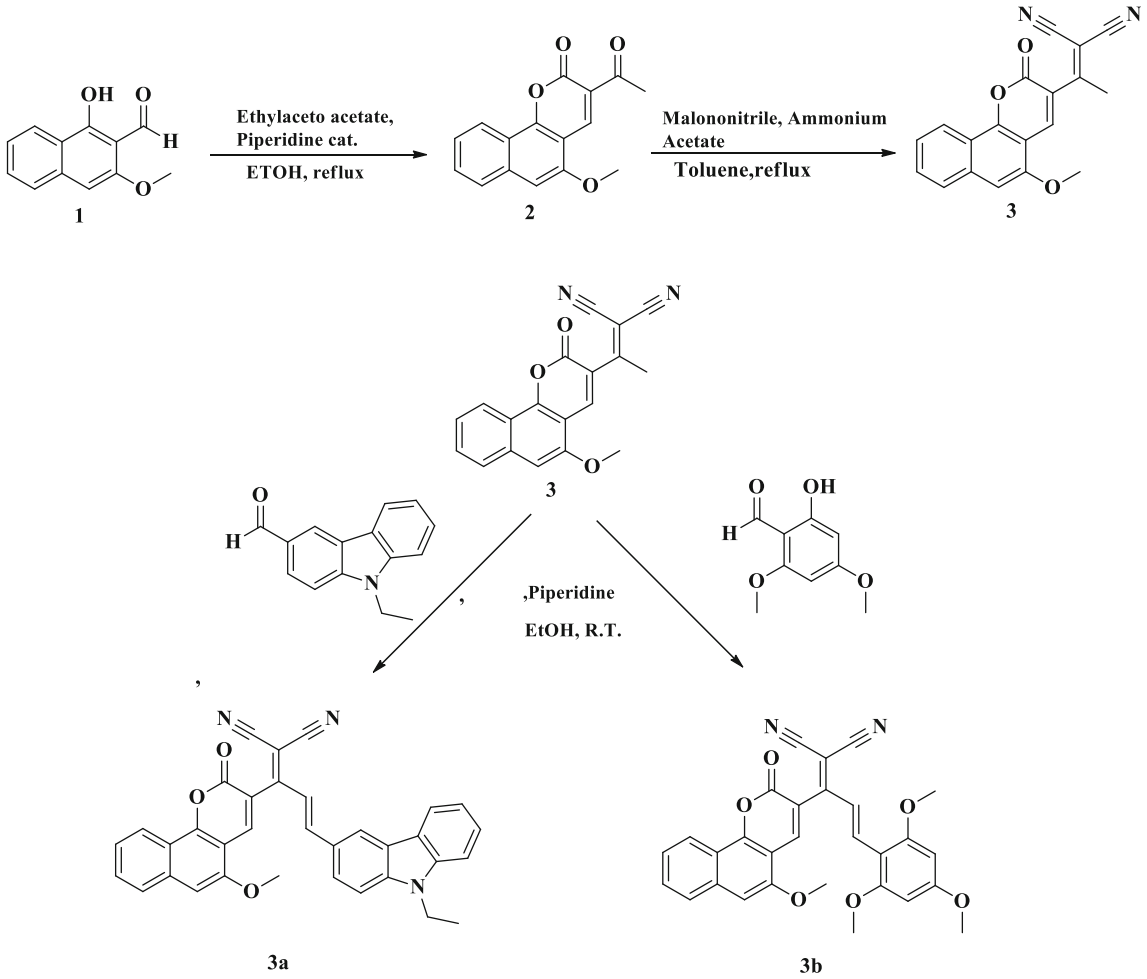

Fig. 2 Synthetic scheme for dye **3a** and **3b**

were recorded on a Perkin Elmer Lambda 25 UV-Visible spectrophotometer; emission spectra were recorded on Varian Inc. Cary Eclipse spectrofluorometer.

All the computations were performed using the Gaussian09 revision D.01 program package [38]. The ground state S_0 geometry and excited state S_1 of the dyes under investigation was optimized in gas phase using DFT method with the help of the functional B3LYP and basis set 6-31G(d) [39–42]. The vibrational frequencies of the optimized structures were computed using the same method to verify the nature of the stationary points. The optimization in the solvent was carried out using the self-consistent reaction field (SCRF) incorporated in the Polarizable Continuum Model (PCM) [43].

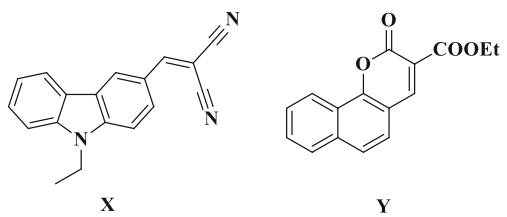

Fig. 3 Structure for controlled dye X and Y

Experimental

Synthesis

The compounds **3a** and **3b** were synthesized by Knoevenagel condensation between compound **3** and donor aldehydes **2a** and **2b** in ethanol using catalytic piperidine at room temperature (25^0 C) which was synthesized from 3-acetyl coumarin **2** whose precursor was 1-hydroxy-3-methoxy-2-naphthaldehyde which was synthesized following the reported method [44].

1-Hydroxy-3-Methoxy-2-Naphthaldehyde (1)

Color: Yellow. Melting Point:175–178^0 C. **^{1}H NMR** (500 MHz, dmso) δ 13.56 (s, 1H), 10.28 (s, 1H),

8.19–8.12 (m, 1H), 7.80–7.72 (m, 1H), 7.68–7.60 (m, 1H), 7.39 (ddd, *J* = 8.3, 6.9, 1.1 Hz, 1H), 6.89 (d, *J* = 18.5 Hz, 1H), 3.94 (s, 3H). **^{13}C NMR** (126 MHz, dmso) δ 194.98, 163.02, 156.72, 138.94, 131.75, 127.36, 124.48, 124.08, 119.94, 107.93, 97.36, 56.37.

Elemental Analysis - Calculated: C, 71.28; H, 4.98; O, 23.74.
Found: C, 71.30; H, 4.98; O, 23.79.

Synthesis of 3-Acetyl-5-Methoxy-2H-benzo[h] Chromen-2-One (2)

A mixture of 1-hydroxy-3-methoxy-2-naphthaldehyde (10 mmol) and ethyl acetoacetate (10 mmol) in 25 ml of absolute ethanol was refluxed in the presence of two drops of piperidine for 30 min. After cooling, the resulting precipitates were recrystallized from ethanol followed by column purification using only toluene to give 3-methoxycoumarin 1a as yellow solid. Colour: Yellow. Yield: 70%. Melting point: 145–150^0 C. **^{1}H NMR** (500 MHz, cdcl$_3$) δ 9.02 (d, *J* = 1.4 Hz, 1H), 8.43 (d, *J* = 8.4 Hz, 1H), 7.73 (d, *J* = 8.2 Hz, 1H), 7.62 (dd, *J* = 8.2, 6.9 Hz, 1H), 7.48 (dd, *J* = 8.3, 7.0 Hz, 1H), 6.91 (s, 1H), 4.04 (s, 3H), 2.77 (s, 3H). **^{13}C NMR** (126 MHz, cdcl$_3$) δ 195.46, 159.28, 154.57, 153.15, 143.82, 136.92, 130.60, 126.86, 125.04, 123.26, 122.10, 118.36, 108.59, 101.07, 55.96, 30.63.

Elemental Analysis - Calculated: C, 71.64; H, 4.51; O, 23.86.
Found: C, 71.06; H, 4.52; O, 23.75.

Synthesis of 2-(1-(5-Methoxy-2-Oxo-2H-benzo[h] Chromen-3-Yl)Ethylidene)Malononitrile (3)

To a solution of coumarin a (0.1 mol) in dry toluene (10 ml) was added malononitrile (0.1 mol), ammonium acetate (2 g) and acetic acid (2 ml). The reaction mixture was heated under reflux using a Dean-Stark water separator until water ceased to be collected. The product obtained was crystallized from ethanol to give the title compound.

Yield: 50% Colour: Light Orange. Melting point: 210–215^0 C. **^{1}H NMR** (500 MHz, cdcl$_3$) δ 9.02 (d, *J* = 1.4 Hz, 1H), 8.43 (d, *J* = 8.4 Hz, 1H), 7.73 (d, *J* = 8.2 Hz, 1H), 7.62 (dd, *J* = 8.2, 6.9 Hz, 1H), 7.48 (dd, *J* = 8.3, 7.0 Hz, 1H), 6.91 (s, 1H), 4.04 (s, 3H), 2.76 (s, 3H). **^{13}C NMR** (126 MHz, cdcl$_3$) δ 171.32, 156.76, 153.08, 151.98, 140.03, 136.32, 130.24, 126.50, 124.88, 122.38, 121.44, 117.93, 111.35, 107.45, 101.20, 87.82, 55.73, 22.33.

Elemental Analysis - Calculated: C, 72.15; H, 3.82; N, 8.86; O, 15.17.
Found: C, 72.11; H, 3.83; N, 8.82; O, 15.18.

General Procedure for Synthesis of Styryls 3a and 3b

A mixture of compound B (1 mmol) and appropriate donor aldehyde (a, b, c or d) (1 mmol) in absolute ethanol in presence of catalytic piperidine was stirred at room temperature for 3 h. The resulting precipitates were purified by column purification using only toluene to give the title compound **3a** or **3b.**

(E)-2-(3-(9-Ethyl-9H-carbazol-3-Yl) -1-(5-Methoxy-2-Oxo-2H-Benzo[h]Chromen-3-Yl) Allylidene)Malononitrile (3a)

Colour: Red. Yield: 51%. M.P.: 278°C. **^{1}H NMR** (500 MHz, cdcl$_3$) δ 8.52–8.48 (m, 1H), 8.43–8.37 (m, 1H), 8.26 (s, 1H), 8.08 (d, *J* = 7.8 Hz, 1H), 7.78 (dd, *J* = 22.4, 8.5 Hz, 2H), 7.66 (dd, *J* = 17.3, 11.2 Hz, 2H), 7.58–7.48 (m, 2H), 7.42 (dd, *J* = 15.9, 8.4 Hz, 2H), 7.31 (dd, *J* = 14.5, 11.5 Hz, 2H), 6.99 (d, *J* = 25.0 Hz, 1H), 4.38 (q, *J* = 7.2 Hz, 2H), 4.05 (s, 3H), 1.47 (t, *J* = 7.2 Hz, 3H). **^{13}C NMR** (126 MHz, cdcl$_3$) δ 164.86, 157.78, 153.37, 152.36, 149.46, 142.33, 141.26, 140.54, 136.38, 130.34, 126.90, 126.75, 125.30, 125.26, 123.77, 123.25, 122.79, 122.74, 120.77, 120.32, 120.06, 119.86, 118.60, 113.54, 112.90, 109.35, 109.17, 108.11, 101.64, 56.06, 37.95, 13.88.

Elemental Analysis Calculated: C, 78.30; H, 4.44; N, 8.06; O, 9.20.
Found: C, 78.31; H, 4.43; N, 8.07; O, 9.21.

(E)-2-(1-(5-Methoxy-2-Oxo-2H-benzo[h] Chromen-3-Yl)-3-(2,4,6-Trimethoxyphenyl) Allylidene)Malononitrile (3b)

Color: Orange. Yield: 70%. M.P.: 290°C. **^{1}H NMR** (500 MHz, dmso) δ 8.53 (d, *J* = 0.9 Hz, 1H), 8.31 (d, *J* = 8.4 Hz, 1H), 7.99–7.94 (m, 2H), 7.73 (dd, *J* = 8.1, 7.0 Hz, 1H), 7.58 (dd, *J* = 8.2, 7.1 Hz, 1H), 7.47 (d, *J* = 15.5 Hz, 1H), 7.39 (s, 1H), 6.28 (s, 2H), 4.03 (s, 3H), 3.86 (s, 3H), 3.79 (s, 6H). **^{13}C NMR** (126 MHz, cdcl$_3$) δ 167.12, 164.85, 162.17, 157.84, 153.20, 152.45, 141.01, 139.41, 136.20, 130.07, 126.82, 125.06, 123.49, 122.76, 120.05, 118.63, 114.00, 113.19, 108.12, 106.74, 101.35, 90.60, 80.04, 55.92, 55.51, 55.01.

Elemental Analysis Calculated: C, 70.44; H, 4.48; N, 5.67; O, 19.41.
Found: C, 70.42; H, 4.47; N, 5.68; O, 19.43.

Result and Discussion

Effect of Solvent Polarity on the Spectroscopic Properties of Dyes 3a and 3b

In order to understand the behavior toward AIE and FMR properties of these dyes, it is important to understand the excited state electronic behavior i.e. charge distribution in the excited state. We have measured the absorption and emission properties in ten different solvents with varying polarity from non-polar to polar solvents. Absorption, emission and other important properties are mentioned in the Figs. 4, and 5 and Table 1. We found that there is not much effect seen on the absorption properties for dye **3a** and **3b**. The only difference is that absorption maxima (λ_{amax}) are red shifted for dye **3a** compared to dye **3b**. This is obvious as carbazole is known to be a strong donor than trimethoxy benzene. Two peaks are evident in the absorption spectra for

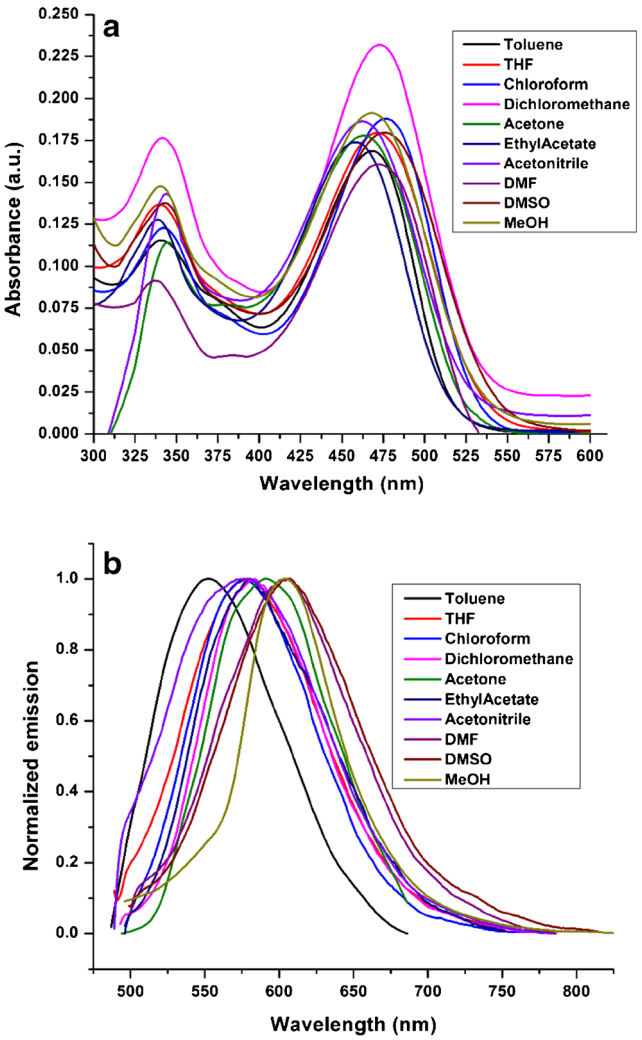

Fig. 4 Effect of solvent polarity on the absorption **a** and emission **b** properties of dyes **3a**

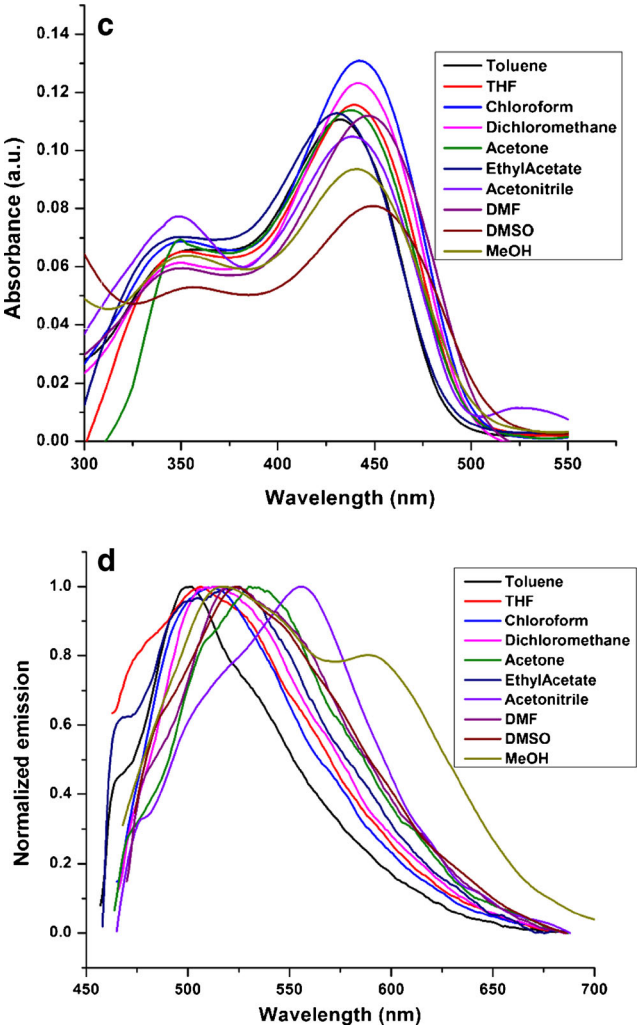

Fig. 5 Effect of solvent polarity on the absorption **c** and emission **d** properties of dyes **3b**

both the dyes. The minor peak is observed at 340–350 nm in all solvents for both dyes which is due to the (π-π* transition). The major peak is the charge transfer (n-π* transition) band which stands at 458–477 nm for dye **3a** and at 430–449 nm for dye **3b** from non-polar to polar solvents. More importantly, the absorption maxima for dye **3a** is red shifted in toluene (468 nm) compared to the control dye X and Y (Fig. 3) which absorbs at 412 nm and 379 nm in acetonitrile respectively. Similarly, the dye **3b** also shows red shifted absorption when compared to controlled dye **Y**. This shows that the coumarin-styryl fusion is advantageous to get red shifted absorption. Emission also drastically shifted to red region when compared to controlled dyes [45, 46].

Emission properties are found to be quite sensitive to the solvent polarity. The emission maxima λ_{emax} for dye **3a** is 558 nm in toluene and 607 nm in DMSO. Similarly the λ_{emax} for dye **3b** is 500 nm in toluene while 555 nm in acetonitrile. This means that though lowest maxima is observed in

Table 1 Experimental photophysical properties of dye **3a** and **3b**

Dye	Solvent	λ^{a}_{max} nm	λ^{b}_{max} ($\times10^4$) cm^{-1}	ε^{c} ($\times10^5$) L mol^{-1} cm^{-1}	f^{d}_{abs}	λ^{e}_{max} nm	λ^{f}_{max} ($\times10^4$) cm^{-1}	$\Delta^{g}\nu$ nm	$\Delta^{h}\nu$ ($\times10^3$) cm^{-1}	S^{i}	$\Delta^{j}\mu_{eg}$
3a	Toluene	468	2.14	0.34	0.39	551	1.81	83	3.22	8201	14.4D
	THF	472	2.12	0.36	0.53	578	1.73	106	3.89	8201	14.6D
	CHCL3	477	2.1	0.38	0.51	576	1.74	99	3.6	8201	14.3D
	DCM	473	2.11	0.46	0.63	582	1.72	109	3.96	8201	14.7D
	Acetone	463	2.16	0.36	0.67	590	1.69	127	4.65	8201	14.8D
	EtOAc	458	2.18	0.35	0.52	563	1.78	105	4.07	8201	14.5D
	Acetonitrile	463	2.16	0.37	0.74	576	1.74	113	4.24	8201	14.9D
	DMF	472	2.12	0.32	0.53	604	1.66	132	4.63	8201	14.8D
	DMSO	476	2.1	0.36	0.55	607	1.65	131	4.53	8201	14.5D
	MeOH	467	2.14	0.38	0.54	604	1.66	137	4.86	8201	14.1D
3b	Toluene	432	2.31	0.22	0.24	500	2	68	3.15	2246	7.5D
	THF	440	2.27	0.23	0.33	506	1.98	66	2.96	2246	7.63D
	CHCL3	442	2.26	0.26	0.32	511	1.96	69	3.05	2246	7.48D
	DCM	441	2.27	0.25	0.31	513	1.95	72	3.18	2246	7.67D
	Acetone	437	2.29	0.23	0.4	532	1.88	95	4.09	2246	7.73D
	EtOAc	430	2.33	0.23	0.28	523	1.91	93	4.14	2246	7.57D
	Acetonitrile	439	2.28	0.21	0.24	555	1.8	116	4.76	2246	7.78D
	DMF	446	2.24	0.22	0.28	520	1.92	74	3.19	2246	7.73D
	DMSO	449	2.23	0.16	0.13	524	1.91	75	3.19	2246	7.61D
	MeOH	440	2.27	0.19	0.18	517	1.93	77	3.38	2246	7.4D

[a] Absorption maxima in nm

[b] Absorption maxima in cm^{-1}

[c] Molar extinction coefficient

[d] Oscillator strength

[e] Emission maxima in nm

[f] Emission maxima in cm^{-1}

[g] Stokes shift in nm

[h] Stokes shift in cm^{-1}

[i] Slope of the Lippert-Mataga plot

[j] Excess dipole moment in Debye (D)

toluene for both the dyes but the solvent giving highest λ_{emax} is different highlighting the variation in the excited state stabilization.

Solvatochromism

We evaluated the ICT character of the two dyes in the solvents by plotting the emission frequency in each solvent versus the relative permittivity of the solvent and the Stokes shift versus the orientation polarizability, that is, the Lippert-Mataga plot respectively [47–49]. Relative permittivity plot can tell how emission wavelength is sensitive to solvent polarity. The plots for dye **3a** and **3b** (Fig. S11 and S12) shows that there is linear increase in the emission maxima with the polarity proving the ICT. Lippert-Mataga plots give the excess dipole moment (difference in the excited state and ground state dipole moment $\Delta\mu_{ge}$ which explains the ICT character of the compound. Thus, the solvent effect of the rotors were studied in detail with Eq. (1), [47, 49] in which $\Delta\nu$ stands for Stokes shift, ν_{abs} and ν_{emi} are absorption and emission maxima in wavenumbers, h is the Planck's constant, c is the velocity of light in vacuum and a is the Onsager cavity radius, and b is a constant. Δf is the orientation polarizability, μ_e and μ_g are the ground-state dipole moment and the excited dipole moment, $(\mu_e - \mu_g)$ is the excess dipole moment respectively, and ε_0 is the permittivity of the vacuum. The dipole moment changes upon photo excitation changes; $(\mu_e - \mu_g)^2$ is proportional to the slope of the Lippert–Mataga plots.

$$\Delta\nu = \frac{\Delta f}{2\pi\varepsilon_0 hca^3}\left(\mu_e - \mu_g\right)^2 + b$$
$$\Delta f = \left(\frac{\varepsilon - 1}{2\varepsilon + 1} - \frac{n^2 - 1}{2n^2 + 1}\right) \quad (1)$$

Based on the emission of the dyes **3a** and **3b** in different solvents, Lippert–Mataga plots were constructed (Fig. S12) which also shows the linearity. The excess dipole moment in case of dye **3a** in solvent DCM and DMF are found to be 14.3 D and 14.8 D (Table 1) respectively. These values for dye **3b** are 7.5 D and 7.7 D respectively in the same solvents. From the Table 1, it is clear that there is substantial charge transfer taking place in the excited state. These values also indicates that **3a** and **3b** are good candidates for FMR and AIE which require high charge transfer. In order to characterize dye **3a** and **3b** by its TICT formation, we plotted the emission frequency against the Rettig function [17, 28]. The linear relation of emission frequency with the Rettig function proves the TICT character of the dyes (Fig. S13).

AIEE Properties for dye 3a and 3b

The AIEE characteristics of the dyes **3a** and **3b** were investigated in a mixture of THF and water (Figs. 9 and 10). In THF dyes **3a** and **3b** were well-dispersed and displayed weak fluorescence in their solution state. To determine whether these dyes have AIEE characteristics, the fluorescence spectra were measured in a series of THF/water mixtures with different volume fractions of water. Since the dyes **3a** and **3b** were soluble in THF but not in water, we added different amounts of water to the pure THF solutions by defining the water fractions (fw) of 0–95% and then monitored the change in the emission wavelength with the excitation wavelengths of 472 nm and 436 nm for dye **3b** and **3b** respectively (Figs. 6 and 7). The concentration was maintained 25×10^{-6} mol L^{-1} throughout all the solutions.

Figures 6 and 7 reveals that both the dyes show highest emission intensity when water fractions (fw) was 95%. In case of both the dyes there is gradual increase in the emission intensity with increase in water fractions from 0 to 60%. But at 80% there is sudden increase in intensity up to 4 fold. This is almost similar at 90% but at 95% there is another 2 fold increase for both the dyes. Another interesting observation is that there is red shift with respect to each water fraction for both the dyes. For dye **3a** there is 70 nm red shift at 95% water fraction compared to 0%. In case of dye **3b** this red shift is 92 nm i.e. from 516 nm to 608 nm. This is the evident demonstration of restricted intramolecular rotation (RIR) and efficient formation of crystal packing responsible for red shifted enhanced emission [8]. It is clear from Fig. 1 that the styryl part in the molecule **3a** is in the plane. That is, the dicyanovinyl part and the carbazole part are in plane and coumarin is out of the plane in the ground state in the THF solution. But in the excited state, the dicyanovinyl and carbazole part are perpendicular to each other. This is the geometrical evidence, why molecule is low emissive in the solution. It is also evident that the geometry

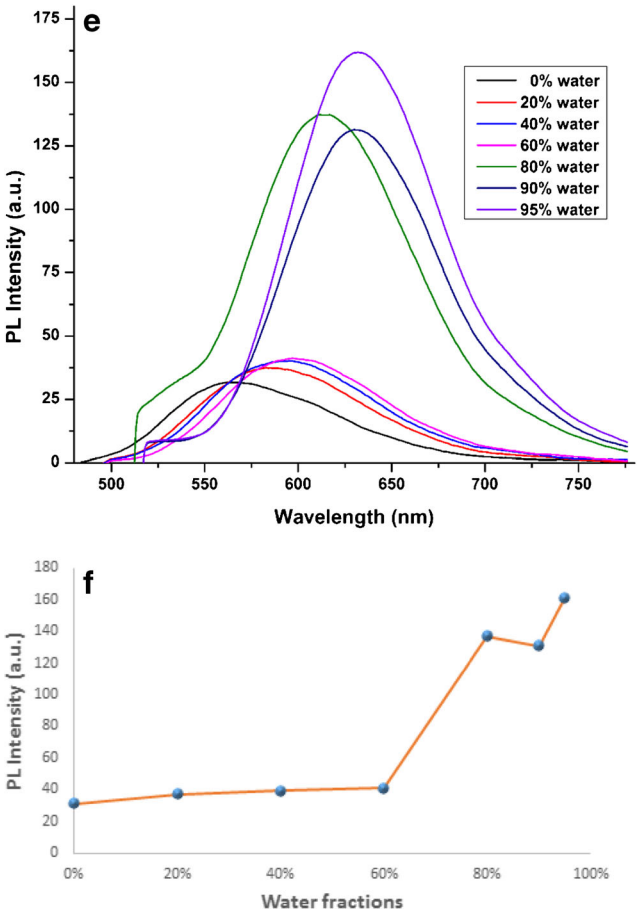

Fig. 6 **e**. PL spectra of the product in THF and THF-Water mixtures with different water fractions (f_w). [**3a**] = 25 μM; λ_{exc} = 472 nm (Slit width – 5 nm, 5 nm). **f**. Plot of the relative PL intensity at 510 nm (I/I0) versus solvent with different water fractions (f_w). I is PL intensity at any f_w, and I0 is the PL intensity measured at f_w = 95%

regarding the coumarin core and dicyanovinyl core is not changing in both states. But the carbazole part is perpendicular to dicyanovinyl part. It shows that due to the rotation of the carbazole unit the charge transfer unit twisting take place and which inhibits the charge transfer. The RIR avoids the excited state twisting which increases the local excited (LE-charge transfer state) state population resulting in the increasing emission intensity. Most of the luminogens show only increase in emission intensity but emission maxima does not change [50, 51]. But in the present case, not only intensity increases but red shift is also observed. The red shift with increasing emission intensity with each increasing water fraction talks about the increase in ICT state. Each water fraction increases the amount of aggregates and with that the population of TICT state is getting lowered as in closed crystal packing, TICT is difficult to occur as rotation is restricted. This might facilitating the increase in charge transfer and lowering the energy of the emissive state. This can be related to the solid state emission also. Dye **3a** which shows

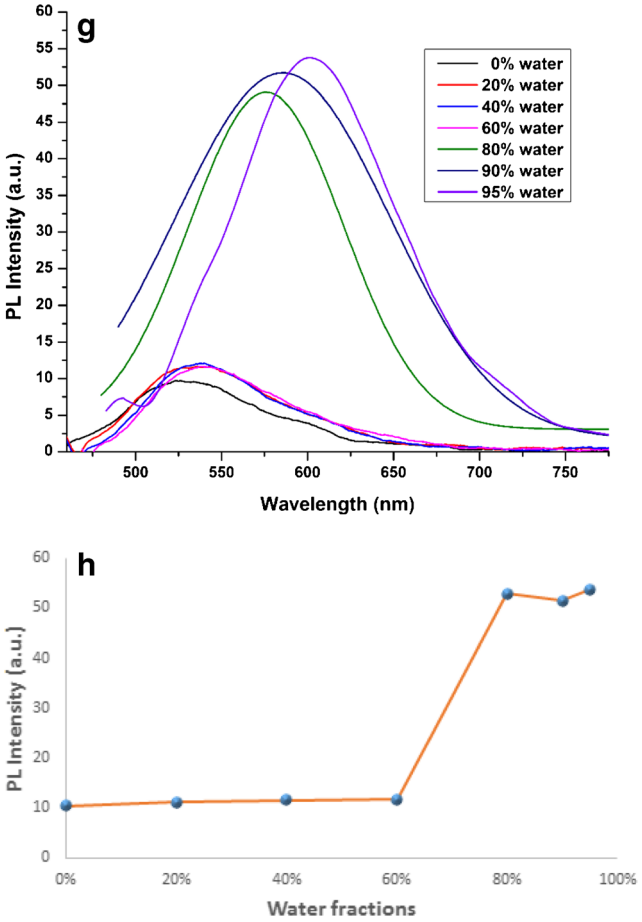

Fig. 7 **g**. PL spectra of the product in THF and THF-Water mixtures with different water fractions (f_w). [**3b**] = 25 μM; λ_{exc} = 436 nm (Slit width – 5 nm, 5 nm). **h**. Plot of the relative PL intensity at 510 nm (I/I0) versus solvent with different water fractions (f_w). I is PL intensity at any f_w, and I0 is the PL intensity measured at f_w = 95%

emission in the orange region in the THF solution shows bright orange-red colour in solid state. Similarly, dye **3b** is bright orange in the solid state but yellow in the THF. It is clear that in solid state as TICT is negligible or almost absent, the emission is red as well as intense. This proves that the arresting of the TICT state in the suitable environment increases the emission characteristics.

Molecular Rotor Properties of Dyes 3a and 3b

In order to act as a molecular rotor for the molecule which measures microenvironment viscosity, its TICT formation in the excited state should be restricted to enhance the emission [9]. This happens as a result of low non-radiative decay via inhibition of TICT. In other words solution viscosity increases emission intensity. We have confirmed the ICT and TICT characteristics of dyes **3a** and **3b** from Lippert-Mataga, Rettig plot and AIEE. To determine whether these dyes have FMR characteristics, the fluorescence spectra of dyes were measured in a series of solvent/PEG 400 mixtures with different volume fractions of PEG 400. We used two solvents of different polarity i.e. DMF as polar solvent and DCM as non-polar solvent. We added different amounts of PEG 400 to the pure DMF or DCM solution by defining the PEG 400 fractions (fp) of 0–95% and then monitored the change in the emission wavelength with the excitation wavelengths of 472 nm for dye **3a** and 436 nm for dye **3b** respectively. From the figures (Figs. 8 and 9), it is clear that, the pattern of increase in emission intensity is the same in both the solvents for both the dyes. The increase in emission intensity is less in DMF:PEG system compared to DCM:PEG system for both the dyes.

The traditional understanding of the FMRs says that the rotors showing sensitivity to the solvent polarity should not show FMR properties, that is, there should not be any increase in emission intensity with increasing viscosity. Our results are contradictory to the old supposition because both systems are giving positive results as FMRs for dye **3a** and **3b**. Previously it was considered that the molecules which does not show solvatochromism are the better FMR candidates. This is because significant ICT facilitate the TICT formation and eventually result in the non-radiative decay instead emission. [23, 52, 53]. Some compounds in the literature are shown to have results which are very similar to us [45] (Fig. 10). Though dye **3a** and **3b** are showing emission solvatochromism and according to old theory should not act as a FMR, they are still showing significant x values. The x values (viscosity sensitivity) for dye **3a** are 0.47 and 0.67 in DCM:PEG and DMF: PEG respectively. In the same system the x values for dye **3b** are 0.21 and 0.34 respectively. These results are really interesting because they prove that it is the polarity of the more viscous solvent is responsible for increase or decrease in the emission intensity. This is because, the compound **5** was failed as FMR in ethylene glycol/glycerol system but showed intensified emission in DCM:PEG 400 system [45]. It is also observed that x values are better in DMF:PEG system though intensity are lower (8 fold) in this system as compared to DCM:PEG (12.2fold) system. This shows that dye **3a** shows more sensitivity in DMF:PEG system than DCM:PEG. Comparing all the x values, it is clear that dye **3a** is more sensitive to solvent viscosity compared to dye **3b.** Another observation is that there is 10 nm blue shift in the emission wavelength in the 95% DMF:PEG system than 0% for dye **3b**. This may due to the lowering % of DMF with each fraction where there is a decrease in the polarity of the medium and slight destabilization of emissive state.

Dye **3a** shows better x values than traditional FMRs DMABN and DCVJ in both systems. The dye **3b** though showed lower values of x compared to **3a** but still can be considered as FMR as x value for dye **3b** in DMF:PEG system

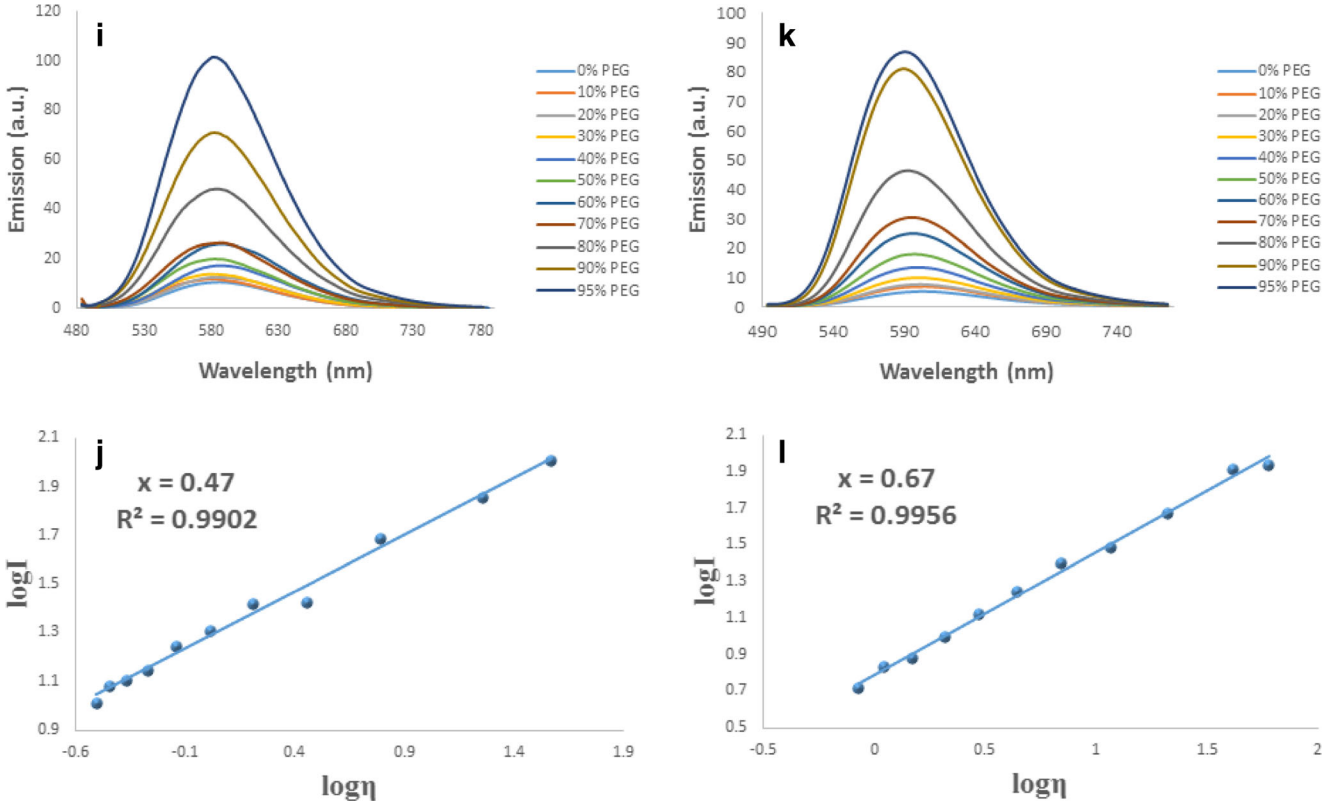

Fig. 8 **i** Emission spectra of dye **3a** in dichloromethane and PEG 400 system. **j** Emission spectra of dye 3a in dmf and PEG 400 system. **k** Dependency of the emission intensity of dye **3a** on the viscosity of the solvents DCM:PEG 400 **l** Dependency of the emission intensity of dye **3a** on the viscosity of the solvents DMF:PEG 400. Concentration = 25 μM, Temperature = 25°C

is 0.39 which very close to 0.41 of DMABN. The differences in the x values in between **3a** and **3b** are obviously due to the power of donating group very similar to the compounds **4** and **5** [45].

The compounds **4** and **5** do not show significant ICT character and fits into the traditional rule. The dye **3a** and **3b** are similar to compound **4** and **5** but shows excellent ICT feature and not fit into the old rule but still show excellent FMR properties. All these observations again proves that compounds sensitive to solvent polarity can also show very good FMR characteristics. Further, viscosity sensitivity depends upon the TICT state whose inhibition or facilitation determines the emission properties of the compound in the solution. The *x* values calculated here are according to a strict mathematical relationship between viscosity η and emission intensity I, known as the Förster-Hoffmann Equation (Eq. 2)

$$\text{Log } I = C + x \log \eta \tag{2}$$

Where C is the temperature dependent constant [54] and *x* is a dye-dependent constant. This relationship has been derived analytically [54–56] and verified experimentally [55, 57].

Conclusion

We have successfully synthesized two 3-styryl benzocoumarins and evaluated their properties on the basis of absorption, fluorescence spectra, aggregation induced emission and viscosity dependent emission. No effect of solvent polarity on absorption spectra is observed but emission properties are found to be solvent polarity sensitive. The dyes have strong ICT and TICT character as proven by the Lippert-Mataga and Rettig plot. The dyes have twisted geometry in the solvent THF as clear from the DFT optimized geometry. Dyes are found to be poorly emissive in the solution state but strongly emissive in the aggregate state as clear form the AIEE study. The restricted intramolecular motion in the aggregate state could be the plausible reason for the enhanced ICT character and eventually the better emission characteristics. Both dyes showed interesting FMR properties as proven by the x values. The restriction of TICT by the restricted intramolecular motion due to viscosity of the solvent system could be the reason for the enhanced emission. The emission intensities of the present rotors are quite evident in the DCM/PEG system compared to DMF/system but the x values are found to be far better in

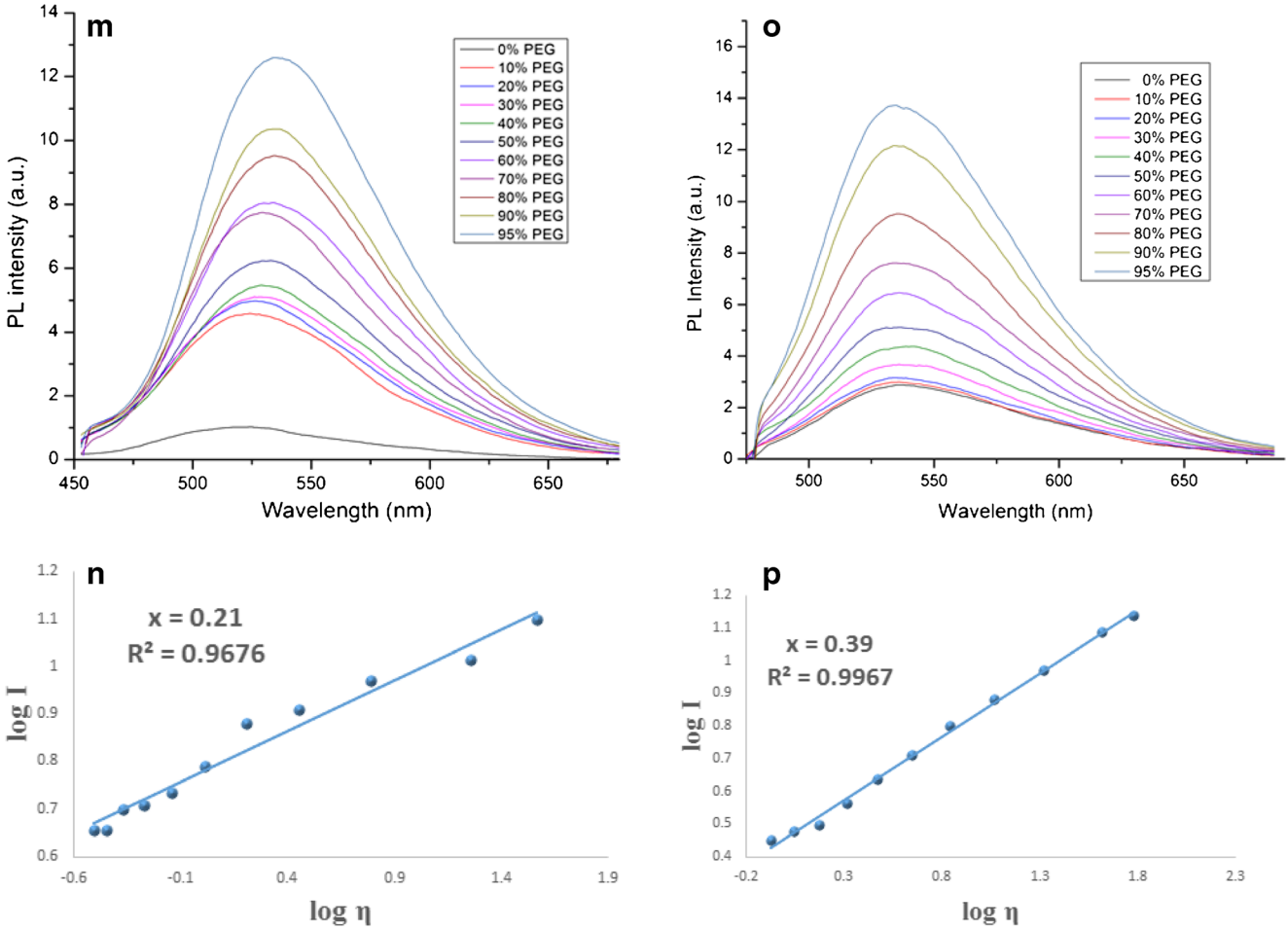

Fig. 9 **m** Emission spectra of dye **3b** in dichloromethane and PEG 400 system. **n** Emission spectra of dye **3b** in dichloromethane and PEG 400 system. **o** Dependency of the emission intensity of dye **3b** on the viscosity of the solvents DCM:PEG 400. **p** Dependency of the emission intensity of dye **3b** on the viscosity of the solvents DMF:PEG 400 Concentration = 25 μM, Temperature = 25 °C

DMF/PEG system. This shows that dyes are more sensitive to more polar viscous system. This is contrary to the traditional concepts of the rotors. This study also proves that the emission enhancement for rotors does not depend completely upon the choice of the solvent. It depends on the geometry of the molecule in the excited state and inhibition of the TICT state to facilitate the ICT state to fluoresce in the given system.

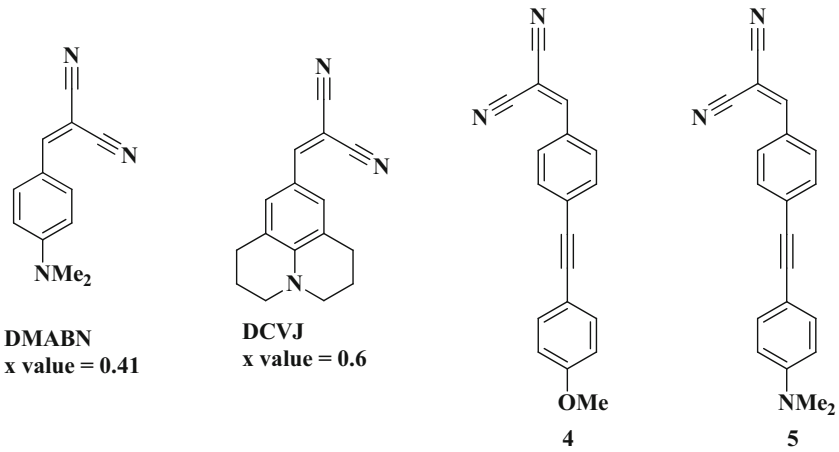

Fig. 10 Some reported FMRs similar to synthesized dyes **3a** and **3b**

Acknowledgements One of the authors, Umesh Warde, is grateful to UGC-SAP, India for Junior and Senior Research Fellowship.

References

1. An B, Kwon S, Jung S, Park SY (2002) Enhanced emission and its switching in fluorescent organic nanoparticles. J Am Chem Soc 124:14410–14415
2. Xu J, Wen L, Zhou W et al (2009) Asymmetric and symmetric dipole-dipole interactions drive distinct aggregation and emission behavior of intramolecular charge-transfer molecules. J Phys Chem C 113:5924–5932. doi:10.1021/jp809258h
3. Haidekker MA, Nipper M, Mustafic A et al (2010) Dyes with segmental. Molecular Rotors, Mobility. doi:10.1007/978-3-642-04702-2
4. Bu F, Duan R, Xie Y et al (2015) Unusual aggregation-induced emission of a Coumarin derivative as a result of the restriction of an intramolecular twisting motion. Angew Chem Int Ed Eng 54: 14492–14497. doi:10.1002/anie.201506782
5. Xiao H, Chen K, Cui D et al (2014) Two novel aggregation-induced emission active coumarin-based Schiff bases and their applications in cell imaging. New J Chem 38:2386. doi:10.1039/c3nj01557b
6. Hong Y, Lam JWY, Tang BZ (2009) Aggregation-induced emission: phenomenon, mechanism and applications. Chem Commun (Camb) 4332–53. doi: 10.1039/b904665h
7. Hu R, Leung NLC, Tang BZ (2014) AIE macromolecules: syntheses, structures and functionalities. Chem Soc Rev 43:4494–4562. doi:10.1039/c4cs00044g
8. Liang J, Tang BZ, Liu B (2015) Specific light-up bioprobes based on AIEgen conjugates. Chem Soc Rev 44:2798–2811. doi:10.1039/c4cs00444b
9. Haidekker MA, Theodorakis EA (2010) Environment-sensitive behavior of fluorescent molecular rotors. J Biol Eng 4:11. doi:10.1186/1754-1611-4-11
10. Wagner BD (2009) The use of coumarins as environmentally-sensitive fluorescent probes of heterogeneous inclusion systems. Molecules 14:210–237. doi:10.3390/molecules14010210
11. Narayanaswamy N, Kumar M, Das S et al (2014) A thiazole coumarin (TC) turn-on fluorescence probe for AT-base pair detection and multipurpose applications in different biological systems. Sci Rep 4:6476. doi:10.1038/srep06476
12. Lichlyter DJ, Haidekker MA (2009) Immobilization techniques for molecular rotors—towards a solid-state viscosity sensor platform. Sensors Actuators B Chem 139:648–656. doi:10.1016/j.snb.2009.03.073
13. Even P, Chaubet F, Letourneur D, Viriot ML, Carré M (2003) Coumarin-like fluorescent molecular rotors for bioactive polymers probing. Biorheology 40:261–263
14. Dong S, Li Z, Qin J (2009) New carbazole-based fluorophores: synthesis, characterization, and aggregation-induced emission enhancement. J Phys Chem B 113:434–441. doi:10.1021/jp807510a
15. Zhang J, Xu B, Chen J et al (2013) Oligo(phenothiazine)s: twisted intramolecular charge transfer and aggregation-induced emission. J Phys Chem C 117:23117–23125. doi:10.1021/jp405664m
16. Yuan WZ, Gong Y, Chen S et al (2012) Fficient solid emitters with aggregation-induced emission and intramolecular charge transfer characteristics: molecular design, synthesis, Photophysical behaviors, and OLED application. Chem Mater 24:1518–1528. doi:10.1021/cm300416y
17. Majenz W, Rettig W (1992) Photophysics of donor-acceptor substituted stilbenes. J Phys Chem 96:9643–9650. doi:10.1021/j100203a016
18. Sasaki S, Drummen GPC, Konishi G (2016) Recent advances in twisted intramolecular charge transfer (TICT) fluorescence and related phenomena in materials chemistry. J Mater Chem C 4:2731–2743. doi:10.1039/C5TC03933A
19. Zachariasse KA, Grobys M, von der Haar T, Hebecker A, Il'ichev YV, Jiang YB, Morawski O, Kühnle W (1996) Intramolecular charge transfer in the excited state. Kinetics and configurational changes. J Photochem Photobiol A Chem 102:59–70.
20. Li Y, Li F, Zhang H et al (2007) Tight intermolecular packing through supramolecular interactions in crystals of cyano substituted oligo(para-phenylene vinylene): a key factor for aggregation-induced emission. Chem Commun (Camb) 1:231–233. doi:10.1039/b612732k
21. Chen J, Law CCW, Lam JWY et al (2003) Restricted intramolecular rotation of 1, 1-substituted 2, 3, 4, 5-Tetraphenylsiloles. Chem Mater 79:1535–1546. doi:10.1021/cm021715z
22. Gao B-R, Wang H-Y, Hao Y-W et al (2010) Time-resolved fluorescence study of aggregation-induced emission enhancement by restriction of intramolecular charge transfer state. J Phys Chem B 114: 128–134. doi:10.1021/jp909063d
23. Jacobson A, Petric A, Hogenkamp D et al (1996) (DDNP): a solvent polarity and viscosity sensitive fluorophore for fluorescence microscopy ⊥. J Am Chem Soc 7863:5572–5579
24. Sharma S, Dhir A, Pradeep CP (2014) ESIPT induced AIEE active material for recognition of 2-thiobarbituric acid. Sensors Actuators B Chem 191:445–449. doi:10.1016/j.snb.2013.10.014
25. Srikrishna D, Dubey PK (2014) Efficient stepwise and one pot three-component synthesis of 2-amino-4- (2-oxo-2 H -chromen-3-yl) thiophene-3-carbonitriles. Tetrahedron Lett 55:6561–6566. doi:10.1016/j.tetlet.2014.10.021
26. Wang X, Li S-Y, Pan Y-M et al (2015) Regioselective palladium-catalyzed decarboxylative cross-coupling reaction of alkenyl acids with coumarins: synthesis of 3-styrylcoumarin compounds. J Org Chem 80:2407–2412. doi:10.1021/jo502572j
27. Min M, Kim Y, Hong S (2013) Regioselective palladium-catalyzed olefination of coumarins via aerobic oxidative heck reactions. Chem Commun (Camb) 49:196–198. doi:10.1039/c2cc37676h
28. Fery-Forgues S, Le Bris MT, Mialocq J-C, Pouget J, Rettig W, Valeur B (1992) Photophysical properties of Styryl derivatives of Aminobenzoxazinones. J Phys Chem 96:701–710
29. Gordo J, Avó J, Parola AJ et al (2011) Convenient synthesis of 3-vinyl and 3-styryl coumarins. Org Lett 13:5112–5115. doi:10.1021/ol201983u
30. Vendrell M, Zhai D, Er JC, Chang Y (2012) Combinatorial strategies in fluorescent probe development. Chem Rev 112:4391–4420
31. Tathe AB, Gupta VD, Sekar N (2015) Synthesis and combined experimental and computational investigations on spectroscopic and photophysical properties of red emitting 3-styryl coumarins. Dyes Pigments 119:49–55. doi:10.1016/j.dyepig.2015.03.023
32. Kovalenko SA (1997) Ultrafast stokes shift and excited-state transient absorption of coumarin 153 in solution. Chem Phys Lett 271: 40–50
33. Sanap AK, Sanap KK, Shankarling GS (2015) Dyes and pigments synthesis and photophysical study of novel coumarin based styryl dyes. Dyes Pigments 120:190–199. doi:10.1016/j.dyepig.2015.04.018
34. Raju BB, Varadarajan TS (1995) Spectroscopic studies of 7-diethylamino-3-styryl coumarins. J Photochem Photobiol A Chem 85:263–267
35. Phadtare SB, Jarag KJ, Shankarling GS (2013) Dyes and pigments greener protocol for one pot synthesis of coumarin styryl dyes. Dyes Pigments 97:105–112. doi:10.1016/j.dyepig.2012.12.001
36. Yeh H, Wu W, Wen Y et al (2004) Derivative of r, −Dicyanostilbene: convenient precursor for the synthesis of Diphenylmaleimide compounds, E - Z isomerization, crystal

structure, and solid-state fluorescence. J Org Chem 69:6455–6462. doi:10.1021/jo049512c
37. Haidekker MA, Theodorakis EA (2007) Molecular rotors — fluorescent biosensors for viscosity and flow. Org Biomol Chem 5: 1669–1678. doi:10.1039/b618415d
38. M.J. Frisch, G.W. Trucks, H.B. Schlegel, G.E. Scuseria, M.A. Robb, J.R. Cheeseman et al (2009) Gaussian 09 Revision A
39. Lee C, Yang W, Parr RG (1988) Development of the Colle-Salvetti correlation-energy formula into a functional of the electron density. Phys Rev B 37:785–789
40. Becke AD (1993) Density-functional thermochemistry. III. The role of exact exchange. J Chem Phys 98:5648. doi:10.1063/1.464913
41. Ditchfield R, Hehre WJ, Pople JA (1971) Self-Consistent Molecular-Orbital Methods. IX. An Extended Gaussian-Type Basis for Molecular-Orbital Studies of Organic Molecules. J Phys Chem 54:724. doi:10.1063/1.1674902
42. Krishnan R, Schlegel HB, Pople JA (1980) Derivative studies in configuration interaction theory. J Chem Phys 72:4654. doi:10.1063/1.439708
43. Cossi M, Barone V, Cammi R, Tomasi J (1996) Ab initio study of solvated molecules: a new implementation of the polarizable continuum model. Chem Phys Lett 255:327–335. doi:10.1016/0009-2614(96)00349-1
44. Pittelkow M, Boas U, Jessing M, Jensen KJ (2005) Role of theperi-effect in synthesis and reactivity of highly substituted naphthaldehydes: a novel backbone amide linker for solid-phase synthesis. Org Biomol Chem 3:508–514. doi:10.1039/b412971g
45. Zhou F, Shao J, Yang Y, et al. (2011) Molecular rotors as fluorescent viscosity Sensors: Molecular Design, Polarity Sensitivity, Dipole Moments Changes, Screening Solvents, and Deactivation Channel of the Excited States. European J Org Chem n/a-n/a. doi: 10.1002/ejoc.201100606
46. Junko M, Ito K (1984) On the spectral properties of some fused 4-Methylcoumarins. Chem Pharma Bull Pharm Bull 32:1178–1182
47. Lakowicz JR (2006) Principles of fluorescence spectroscopy, third. Springer, New York
48. Ji S, Yang J, Yang Q et al (2009) Tuning the intramolecular charge transfer of alkynylpyrenes: effect on photophysical properties and its application in design of OFF-ON fluorescent thiol probes. J Org Chem 74:4855–4865. doi:10.1021/jo900588e
49. Han F, Chi L, Wu W et al (2008) Environment sensitive phenothiazine dyes strongly fluorescence in protic solvents. J Photochem Photobiol A Chem 196:10–23. doi:10.1016/j.jphotochem.2007.11.007
50. Zheng J, Huang F, Li Y et al (2015) The aggregation-induced emission enhancement properties of BF2 complex isatin-phenylhydrazone: synthesis and fluorescence characteristics. Dyes Pigments 113:502–509. doi:10.1016/j.dyepig.2014.09.025
51. Xie Y-Z, Shan G-G, Li P et al (2013) A novel class of Zn(II) Schiff base complexes with aggregation-induced emission enhancement (AIEE) properties: synthesis, characterization and photophysical/electrochemical properties. Dyes Pigments 96:467–474. doi:10.1016/j.dyepig.2012.09.020
52. Haidekker MA, Brady TP, Lichlyter D, Theodorakis EA (2005) Effects of solvent polarity and solvent viscosity on the fluorescent properties of molecular rotors and related probes. Bioorg Chem 33: 415–425. doi:10.1016/j.bioorg.2005.07.005
53. Morimoto A, Biczók L, Yatsuhashi T et al (2002) Radiationless deactivation process of 1-Dimethylamino-9-fluorenone induced by conformational relaxation in the excited state: a new model molecule for the TICT process. J Phys Chem A 106:10089–10095. doi:10.1021/jp0203604
54. Loutfy RO (1986) Fluorescence probes for polymer free-volume. Pure app! Chem 58:1239–1248
55. Forster T, Hoffmann G (2011) (1971) The viscosity dependence of the fluorescence quantum yields of some dye systems. J Phys Chem 75:63–76. doi:10.1524/zpch.1971.75.1_2.063
56. Kung CE, Reed J (1989) Fluorescent molecular rotors: a new class of probes for tubulin structure and assembly. Bochemistry 28: 6678–6686
57. Iwaki T, Torigoe C, Noji M, Nakanishi M (1993) Antibodies for fluorescent molecular rotors. Biochemistry 32:7589–7592. doi:10.1021/bi00080a034